Division for Heliospheric Research

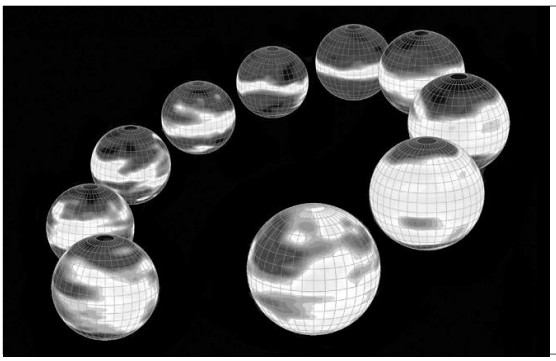

- Solar wind
- Coronal mass ejection
- Interplanetary scintillation
- Global heliospheric structure
- Space weather forecast
- Radio astronomy
- Development of telescopes and instruments
- Pulsar

A supersonic (with a speed of 300–800 km/s) plasma flow, known as the solar wind, emanates from the Sun and permanently engulfs the Earth. While the magnetic field of the Earth acts as a barrier to protect the atmosphere from a direct interaction with the solar wind, a considerable fraction of its vast energy enters the near-surface layer via various processes. Thus, the solar wind acts as a carrier to transfer the Sun's energy to the Earth.

The solar wind varies dramatically with solar activity. In association with eruptive phenomena on the Sun's surface, a high-speed stream of the solar wind sometimes arrives at the Earth and generates intense disturbances in geospace and the upper atmosphere. Space environment conditions that significantly change with the solar activity are known as "space weather," and are currently a topic of significant interest. An accurate understanding of the solar wind is needed to make reliable predictions of space weather disturbances.

We have observed solar wind velocity and density irregularities for several decades using three large antennas to investigate unsolved important issues such as acceleration and propagation mechanisms of the solar wind, space weather forecasting, global structure of the heliosphere, and its variation. In addition, laboratory and fieldwork experiments are performed for improving data quality and upgrading the instruments.

Main Activities in FY2019

Solar wind observations using the IPS system

Broken Fuji antenna structure in March 2019.

We have been performing remote-sensing observations of the solar wind since the 1980s using the multi-station interplanetary scintillation (IPS) system. Tomographic analysis of IPS observations enables the accurate determination of the global distribution of solar wind speed and density fluctuations. IPS observations provide valuable information, particularly for high-latitude solar wind, where in-situ observations are currently unavailable. The IPS system currently consists of three large antennas in Toyokawa, Fuji, and Kiso. The Toyokawa antenna (called the Solar Wind Imaging Facility Telescope) has the largest aperture and highest sensitivity among our three antennas and started daily observations in 2008. The Fuji and Kiso antennas were upgraded in 2013–2014 by installing new low-noise amplifiers, which led to a great improvement in their sensitivity. These two antennas are in mountainous areas and are not used for observations during winter owing to heavy snowfall. The solar wind density fluctuations were derived from Toyokawa IPS observations, measured throughout the year. The IPS data were made available to the public in real time via an ftp server, and were used for various international collaborations, as described below. In March 2019 (i.e., prior to the start of the IPS

observations in this FY), we found that the eastern part of the Fuji antenna reflector had been significantly damaged by snow, and we restored the antenna in April. After finishing the restoration, 3-station IPS observations were conducted until early December. The Fuji IPS observations were briefly interrupted in July by reinforcement work on the antenna. The observation system and network equipment of the Fuji observatory were seriously damaged by lighting on August 1. It took one month to repair this damage, and the Fuji IPS observations restarted on September 1. On November 29, we fixed a misalignment of the Fuji antenna structure which occurred in October and November. We also replaced the driving chains of the Kiso antenna on November 27–28, which had deteriorated owing to long-term operation.

International collaboration for space weather forecast

We performed collaborative research with Dr. B. V. Jackson and his colleagues at the University of California, San Diego (UCSD), on the 3-dimensional reconstruction of the time-varying heliosphere using tomographic analysis of long-term IPS observations. A time-dependent tomography program was developed through this collaborative research, and this program is now available on the NASA Community Coordinated Modeling Center web server, and is running in real time at the Korean Space Weather Center (KSWC) to predict the solar wind reaching the Earth. ISEE has a on research exchange and cooperation agreement with KSWC to promote research on space weather forecasting using IPS data. A combined analysis system using IPS observations and the ENLIL solar wind model was developed to improve space weather forecasting through collaborative research. The UCSD IPS group, represented by Dr. Jackson, won the ISEE Award in this FY, as the UCSD–ISEE collaboration was favorably evaluated.

With the growing awareness of the utility of IPS observations for space weather forecasting, an increasing number of IPS observations have been conducted globally. Besides Japan, Russia, and India, where IPS observations have been conducted for a long time, new dedicated antennas for IPS observations have been constructed in Mexico and Korea, and IPS observations using low-frequency large radio array systems, such as the Low-Frequency Array and the Murchison Widefield Array, have been conducted on a campaign basis. A construction project of a large-aperture antenna dedicated to IPS observations is in progress in China. The integrated analysis of IPS data from these stations enables higher-resolution 3-dimensional reconstructions of the solar wind, which varies rapidly with solar activity. The establishment of WIPSS was proposed at the IPS workshop held in Morelia, Mexico, in 2015. The IPS workshop was held at the Arecibo Observatory in Puerto Rico in December.

Effect of line-of-sight integration in the IPS sky projection map

The Sun-centered sky projection map of g-values derived from IPS observations enables the effective detection of coronal mass ejections (CMEs) propagating in the solar wind, and it has been used in many previous studies. The radial distance of a CME has been determined from the elongation angle between the Sun and the location where the g-value enhancements occur, and CME propagation speed and radial variation have also been addressed using these data. However, CME location on the sky projection map includes the effect of line-of-sight (LOS) integration, and there is a possibility that an apparent change in CME speed may arise from the integration effect. In this FY, we examined the effect of LOS integration on CME location by producing sky projection maps from calculations with a simple CME model. Here, we assumed an axis-symmetrical structure and constant CME speed propagation. We found that the apparent distance of a CME near the Sun becomes smaller than the actual distance when the CME propagation is directed to the Earth, and that the apparent distance approaches the actual distance as the CME moves away from the Sun. This means that the LOS integration brings about an apparent CME acceleration. This effect is remarkable either when the angular width of the CME is small or when the CME expansion speed is non-uniform. Such CME acceleration has seldom been reported from IPS observations, and this implies that the CMEs observed by IPS have a sufficiently wide angular width, and that the apparent acceleration is counterbalanced or overwhelmed by intrinsic deceleration.

Comparative study of the global structures of solar wind and the heliospheric current sheet

The solar wind is composed of a slow wind (~450 km/s) and a fast wind (~800 km/s), known as the bimodal signature of solar wind velocity. These slow and fast winds are the main components of solar wind in the low-mid and high latitudes of the heliosphere, respectively. ISEE-IPS and spacecraft observations have revealed that the boundary latitude of the bimodal structure changes significantly throughout the solar cycle. In this study, we compare the long-term variations of the solar wind structure with the coronal magnetic field structure. The latitudinal structure of the bimodal solar wind is derived from the solar wind synoptic map of each Carrington rotation and compared with the maximum tilt angle of the heliospheric current sheet (HCS), derived from observations by the Wilcox Solar Observatory. The results show that the HCS tilt angle correlates well with the latitudinal average of a solar wind speed of 600 km/s (correlation coefficient 0.8). Since 600 km/s is the average value of the fast and slow wind, the HCS tilt angle is consistent with the latitude of the boundary between the fast and slow wind. The empirical results allow us to estimate the latitudinal structure of the solar wind from the bimodal solar wind velocity after the 1970s, when continuous magnetic field observations of the Sun began.

Solar wind observations using the IPS system

Interplanetary flux ropes (IFRs) are magnetic field structures which are expelled from the Sun into interplanetary space. These ropes have helical magnetic field lines around their central axial field line. To estimate the magnetic field properties of IFRs, force-free IFR models (FF models) are often fitted to *in-situ* observations of IFRs. The Lundquist (cylindrical geometry) and Romashets–Vandas models are often used as FF models. In the fitting of these models, the pitch angle of the magnetic field at the IFR boundary (boundary pitch angle α_p) is conventionally fixed to 90° (conventional method) without sufficient proof. We developed fitting methods in which the assumption that $\alpha_p = 90°$ is relaxed (generalized method) and estimated the difference between the results of the conventional and generalized methods. We found that the fitted axis direction or magnetic flux of IFRs are significantly different between the conventional and generalized methods. From these results, we conclude that the generalized method is more appropriate than the conventional method to estimate the correct magnetic field properties of IFRs.

Model	Significance of effect[a]			
	Axis direction		Magnetic flux	
	γ[b]	β[c]	Φ_t[d]	Φ_p[e]
Lundquist	–	○	○	○
Romashets-Vandas	–	–	○	–

Magnetic field properties of IFRs for which the fitting results of the conventional and generalized methods are significantly different. ○ indicates that the difference is significant. The second and third columns are two angles which determine the axis direction of the IFR. The fourth and fifth columns are two components of magnetic flux.

Estimation of solar coronal density using the Crab pulsar

T Frequency dispersion is observed in the radio waves from a pulsar when we observe them from the Earth. The magnitude of this frequency dispersion (dispersion measure, DM) allows us to estimate the plasma density along the LOS. We have collected remote-sensing measurements of the plasma density of the solar corona using DM data obtained with Toyokawa IPS antenna. Solar wind density significantly drops in response to declining solar activity in some years. This suggests that a remarkable change likely takes place in the solar corona, which is the source region of solar wind. The target of our observations was the Crab pulsar, whose LOS approaches the Sun (to 5 solar radii) every June. Hence, observation of the Crab pulsar enables investigations of the plasma density near the Sun. In addition, the Crab pulsar enables the effective determination of DM, as it emits extremely intense radio waves called giant pulses. From our observations of the Crab pulsar made in June 2018, a marked increase in DM was found around the period of the closest

LOS approach to the Sun. We determined the distribution of the solar corona plasma density by fitting a spherically symmetrical model to the observed DM data. The result was associated with a large error, and one of the causes of this is likely to be the effect of latitudinal/longitudinal variation in the solar corona. To examine this, we analyzed white light data from LASCO coronagraph observations and solar wind speed data from ISEE-IPS observations for June 2018. We found that the streamer associated with the slow wind and the coronal hole associated with the fast wind were located in the equatorial and polar regions, respectively, for the period of our observations, and that the observation point moved from a low-density to a high-density region as the LOS moved away from the Sun. A high DM value observed at a location distant from the Sun (on June 19) is ascribed to the effect of the high-density plasma of the equatorial streamer.

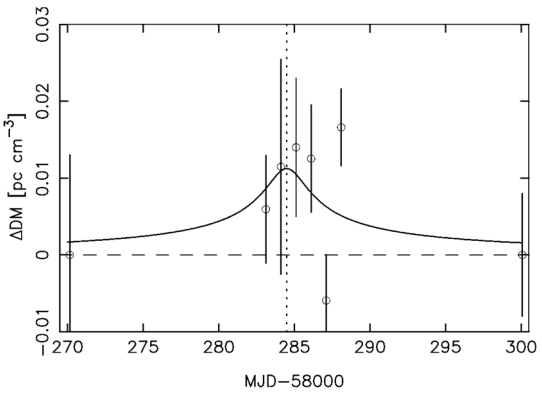

Daily variation of Crab pulsar DM for the period around its closest approach to the Sun. Circles with vertical bars are observed DMs. Solid line represents the best fit model. Vertical dotted line indicates the time of the closest approach of LOS to the Sun.

Validation of CME arrival time forecasted by MHD simulations based on IPS observations

We developed an IPS estimation system, based on a global MHD simulation of the inner heliosphere, to predict the arrival time of CMEs. We demonstrated how the simulation system works using a halo CME event generated by a X9.3 flare observed on September 5, 2017. We found that the CME simulation that best estimated the IPS observations could accurately predict the time of arrival of the CME at the Earth. We validated this system using more than 10 halo CMEs and found that the error in the arrival time is reduced to less than 5 h when using the IPS-based forecasting system. These results suggest that the accuracy of CME arrival time can be improved by including IPS data in our current MHD simulations. Part of this system has been installed in NICT, the space weather forecasting center of Japan, and is used for daily forecasting.

Next-generation interplanetary scintillation observation system

We investigated the design of next-generation IPS observation instruments and developed their pathfinders. To continue IPS observations even in the snowfall season, we considered a flat, two-dimensional phased array with a wide field of view. This structure is also resistant to natural disasters, such as typhoons, as it eliminates the drive unit. A real-time digital signal processing receiver system is required for the digital multi-beam that observes multiple directions simultaneously. This system will enable us to take several all-sky IPS maps within a day to track fast CMEs. It is also able to detect the passage of CMEs and derive their structures by tracking a specific radio source. We designed and developed a low-cost digital board dedicated to IPS observations, using ADCs and FPGAs, and found that it showed adequate performance. The developed prototype can process eight signals simultaneously and has a size of 37 cm × 27 cm, which is a reasonable size for mass-production.